

# CONDITIONING CIRCUIT ANALYSIS FOR SLIMES MANAGEMENT IN QUARRIES

F. BOURGEOIS, G. BAUDET, M. BIZI and H. GABORIAU

*BRGM, Environment and Process Division, Orléans, France*

---

**D**riven by increasingly stringent environmental regulations on water usage, many European quarries are in the process of adding thickening circuits to their wash plants for managing clayey tailings. One of the critical components of this circuit is slurry conditioning. With typical water consumption over 1 m<sup>3</sup> per ton of washed aggregates, quarries produce dilute slime streams that are conditioned with high flocculant dosages to maintain water clarification rates as high as possible. At present, conditioning systems used in the quarrying industry are designed from elementary rules-of-thumb derived from experience. Practitioners acknowledge that conditioning system design criteria should be investigated further in order to design more efficient full-scale conditioning systems. This work focuses on weir-based conditioning tanks used in European quarries. The paper presents an applied analysis of such conditioning systems based on a comparison between a full-scale conditioning circuit and a controlled laboratory conditioning set-up. Within the range of plant operating conditions, this approach shows that full-scale conditioning is essentially governed by average shear rate and conditioning time. However, fine floc size distribution measurements reveal that quarry slimes conditioning is a dynamic process. This explains the high sensitivity of the process to variations in hydrodynamics, and the challenges of industrial conditioning system design.

*Keywords: slimes; conditioning; flocculation; quarry.*

---

## INTRODUCTION

Overall, little information can be found on thickening of quarry waste material as opposed to tailings from metallic (Connelly and Richardson, 1984) and coal preparation (Hogg, 1980; Waters, 1992) plants. The reason for this is that sedimentation in thickeners is the most widely used method for water removal from fine tailings in the mining sector, whereas it is only in recent times that increasingly stringent environmental regulations on water usage have led quarries to start adopting this technology. Considering the high wash water consumption and rising pressures for recycling process water, quarry operators must operate their thickening circuits optimally. There are several possible avenues for improving thickening, one of which is optimization of slurry conditioning. Where thickeners are being used in quarries, flocculant is added to the thickener feed to accelerate clarified water recovery as opposed to the mining sector, where the aim is primarily to maximize solids throughput.

Conditioning efficiency depends on several parameters that offer various scopes for optimization. These include slurry properties (Klimpel and Hogg, 1986), water quality (Rey, 1989), polymer chemistry (Hogg *et al.*, 1993; Spielman, 1977), hydrodynamics (Biggs and Lant, 2002; Spicer *et al.*, 1998; Tomi and Bagster, 1978; Argaman and Kaufman, 1972; Parker *et al.*, 1972; Keys and Hogg, 1979)

and process control (Gregory and Kayode, 1989; Pendse, 1989; Hogg, 1992). Among these parameters, several laboratory investigations (Keys and Hogg, 1979) have shown that the impact hydrodynamics has on conditioning efficiency is paramount. Also, a number of authors (Flesch *et al.*, 1999; Tomi and Bagster, 1978; Argaman and Kaufman, 1972; Parker *et al.*, 1972; Akers, 1975) have proposed comprehensive theoretical analyses of the interaction between hydrodynamic conditions and the flocculation process. Despite this significant body of work, it is fair to say that industrial conditioning system design used in the quarrying industry relies far more on experience than scientific-theories. This situation is partially due to the fact that flocculation research has traditionally favored analysis of flocculation fundamentals in the laboratory over engineering aspects of flocculation at full scale.

Conditioning performance can be defined in a number of ways depending on the aim of the process. With quarry slimes, the principal objective is water clarification. Consequently, clarified water turbidity, floc subsidence rate and floc size distribution (Farrow *et al.*, 2000; Biggs and Lant, 2000) are relevant indicators of conditioning efficiency.

## METHODS AND MATERIALS

Weir-based conditioning tanks (see Figure 1) provide a favorable environment for conditioning mineral slurries in

## CONDITIONING CIRCUIT ANALYSIS

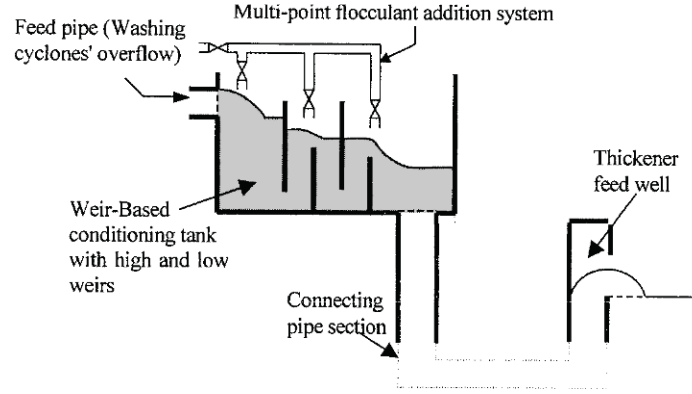


Figure 1. Schematics of a quarry slimes conditioning system.

quarries. This gravity-driven conditioning system consists of a conditioning tank with high and low weirs followed by a series of connecting pipes that feed the thickener. Emphasis is placed on the overall conditioning system including both the conditioning tank and the connecting pipe section.

The 2 m<sup>3</sup> conditioning box presented in Figure 1, which is operating at a 220 t h<sup>-1</sup> quarry in the northwestern part of France, is divided into compartments delimited by individual flocculant injection points. The design of the tank is such that the slurry has to go around a number of low and high weirs. The height of and spacing between weirs are calculated based on a maximum flow velocity set point inside the conditioning tank. The design rationale consists of delivering a high mixing energy input per unit volume of slurry without developing regions of high shear rates.

A basic circuit analysis was carried out for the nominal slurry flow rate  $Q_f = 0.106 \text{ m}^3 \text{ s}^{-1}$  and slurry density  $\rho_p = 1022 \text{ kg m}^{-3}$ . The absolute slurry viscosity  $\mu_p$  was calculated using Heiskanen and Laapas' (1979) viscosity model for an average floc porosity of 0.96. Such a value was obtained by applying a fractal analysis to floc size distributions obtained with a dedicated laser sizer. The slurry, which consists of washing cyclones' overflow, had a  $d_{80} = 80 \text{ }\mu\text{m}$ .

Analysis of the conditioning system starts with estimation of volumes and residence times. The volumes of individual compartments (cf. Table 1) were estimated by measuring free surface heights during operation. The head loss  $h$  between adjacent compartments was obtained directly by measurement of the free surface height drops from one compartment to the next. Free surface height drops between adjacent compartments 1, 2 and 3 were 0.23, 0.20 and 0.22 m, respectively. A standard analysis of major and minor losses yielded a head loss  $h = 0.52 \text{ m}$  in the 13 m long pipe section.

Next is a series of hydrodynamic parameters (Akers, 1975) that can be used for characterizing the

hydrodynamic environment during conditioning from first hand observations:

- the power  $P_b$  (Wt) dissipated across a given head loss  $h$ :

$$P_b = \rho_p \times Q_f \times h \times g \quad (1)$$

where  $g$  is the gravitational acceleration.

- the average shear rate  $\bar{G}$  (s<sup>-1</sup>):

$$\bar{G} = \sqrt{\frac{P_b}{V \times \mu_p}} \quad (2)$$

- the product between average shear rate and residence time  $\bar{G} \times \tau$  (dimensionless);
- the maximum shear rate  $G_{\max}$ —there is no available formula for calculating maximum shear rate inside weir-based conditioning tanks; this information could be obtained by laser doppler velocimetry or CFD simulation, however such techniques are not readily available in practice; it is likely that areas of high shear will occur in the vicinity of low weirs where local contractions might develop;
- the volume specific energy input  $E_s$  (J m<sup>-3</sup>):

$$E_s = \frac{P_b \times \tau}{V} \quad (3)$$

- the micro-turbulence length  $\lambda$  (m) (Spielman, 1977):

$$\lambda = \left( \frac{\mu_p^3 V}{\rho_p^2 P_b} \right)^{1/4} \quad (4)$$

- this turbulence length is related to the mechanical power expanded per unit volume of slurry; it is caused by the energy-containing eddies that carry and dissipate most of the fluid's kinetic energy;
- the macro-turbulence  $\Lambda$  (m)—essentially a function of geometry (Tomi and Bagster, 1978), there is no known

Table 1. Basic hydrodynamic analysis of a full-scale quarry conditioning system.

Sections	Volume $V$ (m <sup>3</sup> )	Residence time $\tau$ (s)	$P_b$ (W)	$\bar{G}$ (s <sup>-1</sup> )	$E_s$ (J m <sup>-3</sup> )	$\lambda$ ( $\mu\text{m}$ )
Compartment 1	0.605	5.7	244	465	2310	63
Compartment 2	0.479	4.5	213	487	2003	61
Compartment 3	0.531	5.0	234	485	2207	61
Connecting pipe section	1.388	13.1	449	416	4231	66

analytical method for estimating the macro-turbulence in the geometry of interest.

Finally, Table 1 shows the conditioning parameters that characterize the conditioning system shown in Figure 1.

Several observations can be made from this rudimentary analysis. Firstly, it is found that the system achieves a gradual injection of mechanical power into the slurry during conditioning. This leads to a fairly uniform average shear rate throughout the system. Secondly, the micro-turbulence length appears to be commensurable with the top particle size from quarry slimes, hence it is favorable in terms of particle collision probability and floc formation (Tomi and Bagster, 1978). Thirdly, Table 1 highlights the significance of the connecting pipe section, which is responsible for 39% of the overall power expanded within the conditioning system as a whole. As earlier mentioned, there is no simple way of estimating maximum shear rate and macro-turbulence in such a system.

Thus far, a basic hydrodynamic analysis of weir-based conditioning systems used in quarries has been carried out from simple site observations. Yet, the relative influence of hydrodynamic parameters is not obvious to the practitioner.

Minus 80  $\mu\text{m}$  fines produced at a washing plant near Orléans (France) were used in series of flocculation tests conducted at full scale and laboratory scale in order to compare hydraulic and conventional conditioning. The principal minerals in the slurry were illite (13 wt%), smectite, sepiolite and attapulgite (23 wt%), kaolinite (9 wt%), calcite (31 wt%), feldspars and mica (15 wt%) and quartz (5 wt%).

## RESULTS AND ANALYSES

In order to analyse the behavior of such industrial conditioning systems further, it was decided to explore the direct link between conditioning at full scale in a weir-based tank and under controlled laboratory conditions.

### Laboratory Conditioning Set-up

A flat-bottom baffled geometry was selected as the basis for laboratory conditioning experiments. The geometry is

given in Figure 2(a) in dimensionless form. The vessel contained four regularly spaced baffles. Vessels with inner volumes of 0.5, 4 and 50 l were used during this work.

The selected impeller was a two-blade radial flow turbine. Torque readouts from the mechanical stirrer were calibrated with water and a 50 wt% sucrose solution at 20°C. The resulting power curve (Penney, 1985) is shown in Figure 2(b). This power curve was used to determine the torque  $T$  and rotational velocity  $N$  that would dissipate a given power  $P_b$  during conditioning.

With such a set-up, the micro-turbulence length follows equation (4), hence it is inversely proportional to  $N^{1/2}$ . In such a configuration, it is admitted that the macro-turbulence length, which depends on geometry only, equals  $0.1 \times D$  (Tomi and Bagster, 1978) for a given power  $P_b$ . With a 4 l vessel, one finds  $\Lambda \approx 7$  mm.

### Direct Comparison Between Plant and Laboratory Conditioning Systems

A 2 m<sup>3</sup> conditioning tank that differed slightly from Figure 1 was commissioned and connected to the plant washing cyclones' overflow via a gate valve. The basic geometry of this tank is shown in Figure 3. A single flocculant addition point was used during site trials and samples of flocculated suspension were grabbed in the middle of the second compartment. Control over the conditioning tank feed rate with the gate valve permitted varying the amount of power  $P_b$  expanded into the slurry between flocculant injection point A and sampling point location B.

During site trials, the slurry solids concentration remained stable around a set point of 8 kg m<sup>-3</sup>. For each flow rate, the water head loss across the first high weir was measured for calculation of the mixing parameters reviewed above. With the inlet being placed at the base of the tank, the kinetic energy of the incoming flow had to be accounted for in order to quantify the power dissipated between points A and B. The flocculant used on site and in the laboratory was SNF AN934 MPM, a medium molecular weight slightly anionic acrylate-acrylamide co-polymer. Given that the flocculant feed solution of 0.5 g l<sup>-1</sup> could only be added through

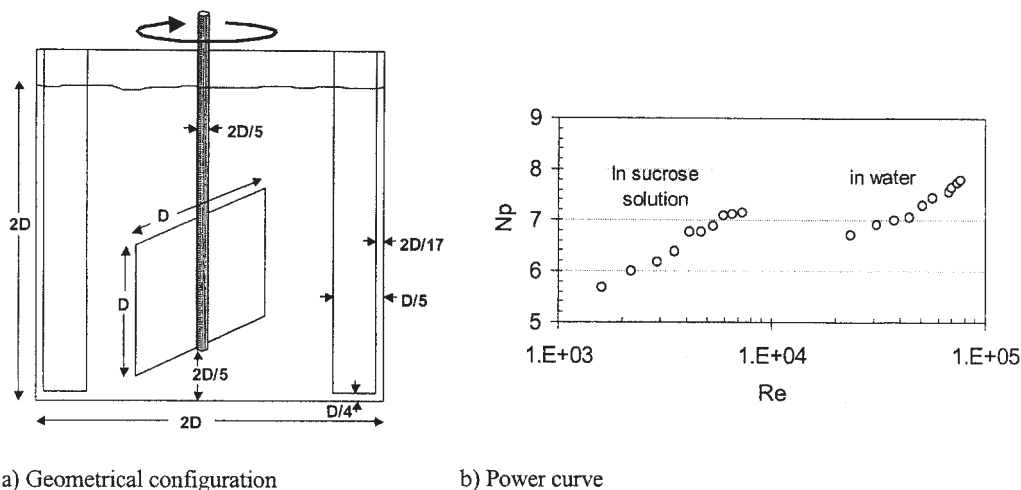


Figure 2. Laboratory conditioning system.

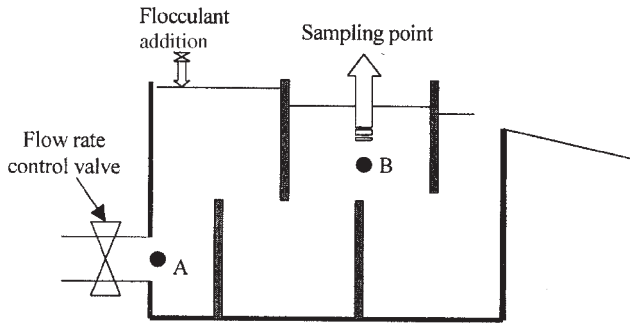


Figure 3. Operating and sampling procedure of a full-scale conditioning tank.

spargers at a fixed flow rate, the actual flocculant dosage varied with feed rate into the conditioning tank (cf. Table 2).

Samples of conditioned slurry were grabbed by carefully dipping a 21 graduated glass cylinder directly into the conditioning tank at the sampling point location B indicated in Figure 3. Immediately after filling the graduated cylinder, it was carefully placed in upright position and floc settling velocity was measured by tracking falling flocs by eye and timing their rate of descent down the cylinder. Likewise, floc settling velocity distributions were obtained for three tank feed rates. Clarified water samples were collected 5 min after the end of floc settlement for measurement of supernatant turbidity. Table 3 summarizes the operating conditions, conditioning parameters and conditioning performance for the three feed rates tested at full-scale.

In order to compare these results with laboratory conditioning tests conducted with the same conditioning power  $P_b$  and time  $\tau$ , flocculation tests were conducted with a 4 l laboratory conditioning vessel. Conditions used, which are reported in Table 3 included those of the three feed flow rates tested on site (cf. shaded columns in Table 3), plus a number of intermediate conditions that would correspond to intermediate feed rates into the full-scale tank, keeping in mind that both residence time and flocculant dosage varied with feed rate. In order to match plant operating conditions as closely as possible, laboratory tests were conducted using plant process water. The flocculant type was SNF AN934 MPM as in the plant. Finally, the flocculant makeup process followed the manufacturer's guidelines that were also used on site. In each case, flocculant was squirted into the slurry using graduated syringes. The conditioning settings used in the laboratory are given in Table 3.

From literature (Farrow and Warren, 1993) and experience, the authors have found that it is difficult to transfer

flocculated suspensions from one vessel into another without degrading the flocs. As a result, settling experiments were carried out directly inside the conditioning vessel. The experimental procedure consisted in stopping the impeller at the end of the conditioning time and let the flocs settle directly inside the conditioning tank, thereby leaving flocs totally undisturbed. Floc settling was captured by video with a standard  $640 \times 480$  CCD camera. Settling velocity measurements were obtained from analysis of the videos.

Figure 4(a) and (b) shows turbidity and floc settling rate measurements for both plant and laboratory scales. It is found that clarified water turbidity results obtained in the laboratory agree with those measured on site. Controlled laboratory tests do therefore yield satisfactory prediction of full-scale water clarification of quarry slimes within the range of  $\bar{G}$  and  $\tau$  values achieved industrially.

At conditioning settings corresponding to  $\bar{G} > 230 \text{ s}^{-1}$ , the predictions of floc settling velocity obtained in the laboratory matched those measured on site. This confirms that hydrodynamic conditions that impact floc formation do match for the two systems for the same doublet ( $\bar{G}$ ;  $\tau$ ). Below  $230 \text{ s}^{-1}$ , it is found that laboratory conditioning test results no longer match those obtained at full scale. Even though there is one single measurement point at full-scale at  $180 \text{ s}^{-1}$ , the confidence intervals leave no doubt about the significance of the discrepancy. The origin of this discrepancy is not yet explained, however it is attributed to the dynamic nature of quarry slimes conditioning and its high sensitivity to other hydrodynamic parameters such as the maximum shear rate  $G_{\max}$ .

### Insights into the Dynamic Nature of Quarry Slimes Conditioning

A series of conditioning tests, at a flocculant dosage of  $168 \text{ g t}^{-1}$ , were carried out in the 4 l conditioning vessel at constant  $\bar{G}$ , constant  $\tau$  and constant  $\bar{G} \times \tau$  for a power input of 43 W. Floc size distributions were obtained using a Master Sizer S (long bed) equipped with a 10 mm inner width glass cell. Using low angle scattered intensity, the high focal length can analyse floc sizes from  $4 \mu\text{m}$  up to  $3500 \mu\text{m}$ . The cell is gravity fed so as to reduce shear stresses applied to the flocs. Experimental measurements of supernatant turbidity, maximum floc size  $d_{99}$  and normalized density size distributions of the flocs are represented in Figures 5 and 6. Deconvolution of multimodal density size distributions yielded two or three log-normal subpopulations

Table 2. Conditioning results obtained at full-scale for three operating feed rates.

Conditioning properties between points A and B (cf. Figure 3)	Conditioning tank feed rate ( $\text{m}^3 \text{h}^{-1}$ )		
	186	222	270
Flocculant dosage ( $\text{g t}^{-1}$ )	202	168	139
Solids content ( $\text{kg m}^{-3}$ )	8	8	8
$P_b$ (W)	43	73	131
$\bar{G}$ ( $\text{s}^{-1}$ )	177	228	298
$\tau$ (s)	17.8	15.3	13.2
Floc settling velocity ( $\text{m min}^{-1}$ ) <sup>a</sup>	$1.961 \pm 0.570$	$0.845 \pm 0.308$	$0.338 \pm 0.084$
Clarified water turbidity (NTU)	100	105	150

<sup>a</sup>Precision equals twice the experimental standard deviation.

Table 3. Conditioning settings used in the laboratory conditioning experiments.

Conditioning properties between points A and B (cf. Figure 3)	Equivalent conditioning tank feed rate ( $\text{m}^3\text{h}^{-1}$ ) <sup>a</sup>										
	161	173	186	198	210	222	238	254	270	285	301
Flocculant dosage ( $\text{g t}^{-1}$ )	233	216	202	189	178	168	157	148	139	131	124
Solids concentration ( $\text{kg m}^{-3}$ )	8	8	8	8	8	8	8	8	8	8	8
$P$ (W)	28	35	43	52	62	73	90	109	131	155	182
$\bar{G}$ ( $\text{s}^{-1}$ )	144	160	177	195	210	228	251	274	298	322	347
$N$ (rpm)	92	98	105	112	118	124	133	141	149	157	165
$\tau$ (s)	20.1	19	18	17	16	15	14	14	13	13	12

<sup>a</sup>Italic columns correspond precisely to the conditions tested at full scale.

of flocs whose characteristics reflect the dynamics of floc growth and floc breakage.

Above all, these results demonstrate that the short conditioning times used in the quarrying industry imply fast kinetics and conditions far remote from those that can lead to a stable maximum floc size in a stress field governed by  $\bar{G}$ . Hence, quarry slimes conditioning is an utterly dynamic process. This means that using a given value of  $\bar{G}$  cannot be sufficient for the laboratory system to completely match the performance of the full-scale conditioning system, nor is it a reliable basis for designing full-scale conditioning systems.

Together, Figures 5 and 6 highlight most of the mechanisms involved in slimes conditioning. Before proceeding further, it is important to note that Figure 6 reveals the existence of two basic populations of flocs whose mode size and volume fraction are totally inter-connected and extremely sensitive to changes in hydrodynamic conditions. The analysis of the interactions between these two distinct populations reveals interesting features about the dynamic nature of quarry slimes conditioning.

In the range of  $\bar{G}$  and  $\tau$  values achieved in full-scale conditioning systems, it can be observed that the evolution of these populations of flocs follows antagonistic mechanisms of the flocculation process:

- the first mechanism is the aggregation of particles then of small flocs for which medium values of  $\bar{G}$  yield a monotonic increase in the rate of both particle capture and floc growth;
- the second mechanism involves both breakage and erosion of large flocs. This floc degradation process increases with  $\bar{G}$ ,  $\tau$  and floc size. If the value of  $\bar{G}$  exceeds the detachment shear strength for particles or

for small flocs from the surface of large flocs, or if  $\bar{G}$  is higher than the shear strength of large flocs, the maximum floc size decreases with both  $\bar{G}$  and  $G_{\text{max}}$ .

At a constant conditioning time ( $\tau = 15.3$  s), the concomitant increase in the mode size of the population of large flocs, their maximum size  $d_{99}$ , their volume fraction and the decrease in supernatant turbidity and volume fraction of small flocs when  $\bar{G}$  goes from 100 to  $600\text{ s}^{-1}$  clearly illustrate this mechanism. The second mechanism is revealed by the finer mode size of the small flocs' population at higher  $\bar{G}$  values. This reduction in the mean size of the small flocs corresponds to the birth of a second population of small flocs whose mode is less than that of the single primary floc population formed at short conditioning times. Indeed, Figure 6(a) clearly shows that a short conditioning time ( $\tau = 5$  s for  $\bar{G} = 228\text{ s}^{-1}$ ) that is close to the theoretical mixing time yields a single population of small flocs. It is only for longer conditioning times that large floc formation is observed. The second small floc population is the probable result of erosion of the large floc population. The measured increase in both  $d_{99}$  and the mode size for the large floc population with  $\bar{G}$  is indicative of an aggregation mechanism. However, Figure 6(b) shows a reduction of the width of the large floc population' distribution when it is unique and the birth of a second population of large flocs whose mode size is less than that of the population formed at lower  $\bar{G}$  values. These observations confirm that large flocs are also subjected to a breakage mechanism at higher  $\bar{G}$  values.

At an intermediate constant  $\bar{G}$  value ( $228\text{ s}^{-1}$ ), the increase in conditioning time from 5 to 50 s leads to:

- The birth of a population of large flocs generated by aggregation of small flocs from the unique log-normal

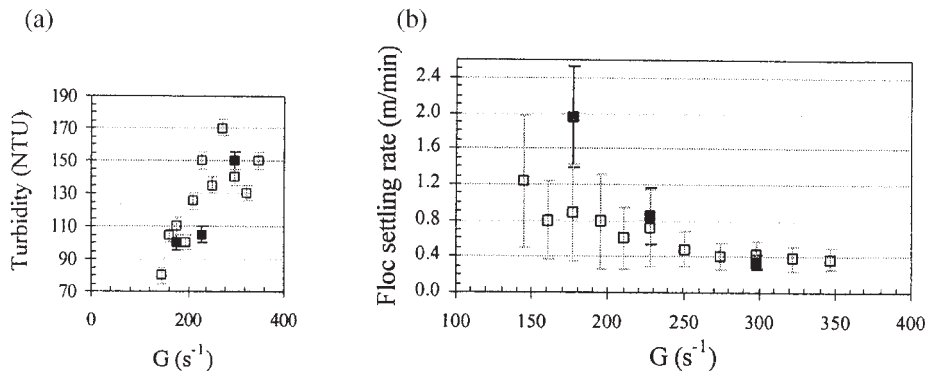


Figure 4. Comparison between full-scale (solid symbols) and laboratory conditioning systems (empty symbols). (a) Supernatant turbidity; (b) floc settling rate distribution.

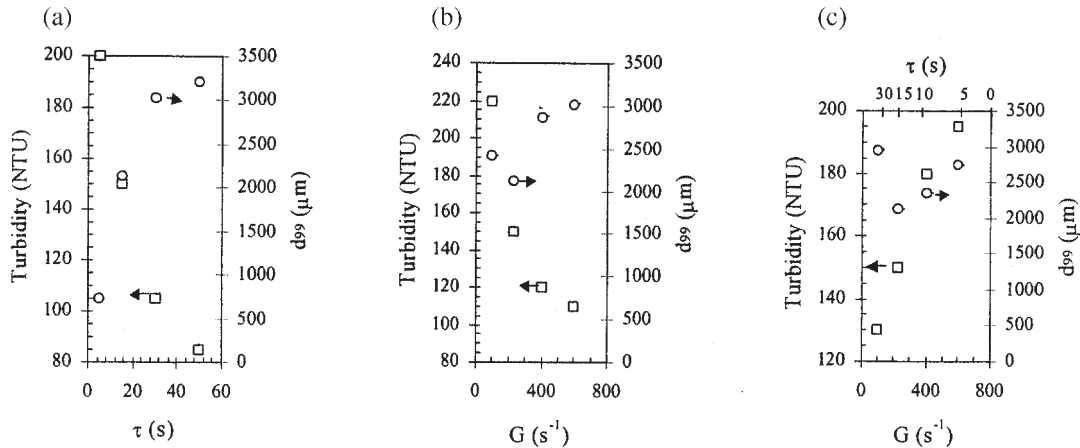


Figure 5. Sensitivity of quarry slimes conditioning to variations in  $\bar{G}$ ,  $\tau$  and  $\bar{G} \times \tau$ . Flocculant dosage:  $168 \text{ g t}^{-1}$ . (a)  $\bar{G} = 228 \text{ s}^{-1}$ ; (b)  $\tau = 15.3 \text{ s}$ ; (c)  $\bar{G} \times \tau = 3500$  ( $100 \text{ s}^{-1} < \bar{G} < 600 \text{ s}^{-1}$ ;  $6 \text{ s} < \tau < 35 \text{ s}$ ).

population (mode =  $171 \mu\text{m}$  in Figure 6a) obtained by aggregation of the initial particles and micro-flocs. The reduction of the small flocs' volume fraction and the increase in the volume fraction of the large floc population are clearly connected, large flocs growing at the expense of small flocs. Globally, the increase in  $d_{99}$ , large floc volume fraction and size of the large floc population indicate a continuous aggregation process with conditioning time at a moderate  $\bar{G}$  value. However, the relatively low increase in the mode size between 30 and 50 s, combined with the birth of a second population of large flocs, are further proofs of the competing effects of breakage and erosion mechanisms for the large flocs. Compared with the effect of  $\bar{G}$ , the moderate reduction in the mode size of the small floc population indicates that less erosion is taking place, which is a consequence of the moderate  $\bar{G}$  value used to test the effect of conditioning time.

- A reduction in supernatant turbidity. This trend confirms an aggregation process for the residual initial particles and the micro-flocs responsible for water turbidity.

At a moderate constant value of the dimensionless product  $\bar{G} \times \tau$  ( $=3500$ ), conditioning times are very short

at high values of  $\bar{G}$  (400 and  $600 \text{ s}^{-1}$ ). These short conditioning times are not sufficient for residual particles and micro-flocs to aggregate and form small or large flocs. This effect is particularly significant given the low solids concentration ( $8 \text{ g l}^{-1}$ ) typical of quarries and the significant proportion of colloidal clayey minerals with high structural charge (e.g. montmorillonite). As a result, supernatant turbidity increases with  $\bar{G}$ . The lower maximum floc size for  $\bar{G} = 228 \text{ s}^{-1}$  and  $\tau = 15.3 \text{ s}$  indicates that  $\bar{G} = 100 \text{ s}^{-1}$  and  $\tau = 35 \text{ s}$  is a more efficient combination of  $\bar{G}$  and  $\tau$  in terms of turbidity and floc size. For  $\bar{G} = 100 \text{ s}^{-1}$ ,  $\bar{G}$  has a purely positive effect on  $d_{99}$ , whereas  $\tau$  has a purely negative effect on turbidity and a positive effect on  $d_{99}$ . With  $\bar{G} = 228 \text{ s}^{-1}$  and  $\tau = 15.3 \text{ s}$ , the increase in  $\bar{G}$  is not sufficient to compensate for the reduction in  $d_{99}$  caused by the relatively short conditioning time. For other combinations of  $\bar{G}$  and  $\tau$ , the increase in  $\bar{G}$  is sufficient to offset the lower conditioning times, leading to a moderate increase in  $d_{99}$ . Overall, these experimental observations highlight the complex interaction between  $\bar{G}$  and  $\tau$ .

More experimental work is necessary to fully characterize the interaction between  $\bar{G}$  and  $\tau$ . However, the complexity of the interactions brought to light by this work is enough to

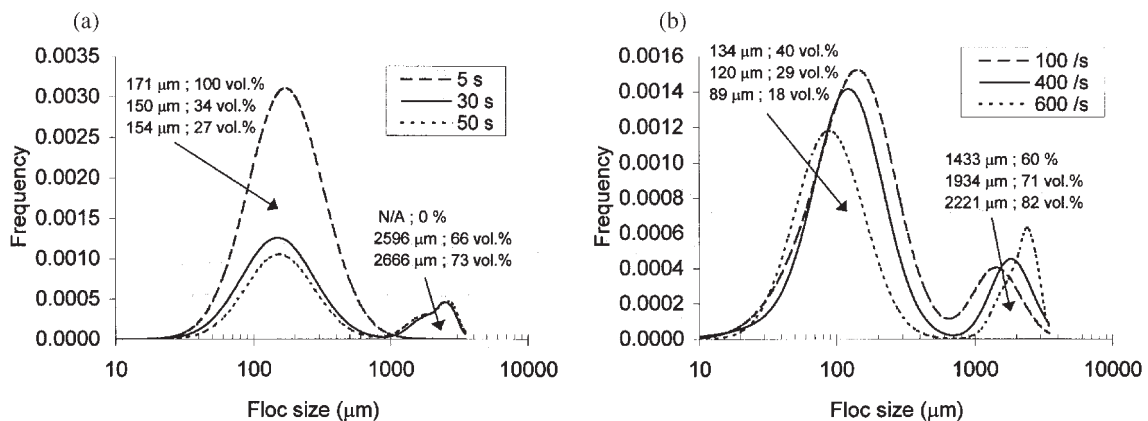


Figure 6. Sensitivity of floc size distribution to variations in  $\bar{G}$  and  $\tau$  (values shown represent the mode and volume fraction of the small and large floc populations). Flocculant dosage:  $168 \text{ g t}^{-1}$ . (a)  $\bar{G} = 228 \text{ s}^{-1}$ ;  $\tau$  variable. (b)  $\tau = 15.3 \text{ s}$ ;  $\bar{G}$  variable.

conclude that the dimensionless product  $\bar{G} \times \tau$  does not make a suitable design criterion for slimes conditioning system design.

This work has shown that laser sizing, given an appropriate design and a carefully controlled experimental protocol, is capable of providing measurements of floc size distributions that are extremely sensitive to changes in hydrodynamic conditions. Additional work is currently under way to unravel the effects of other important hydrodynamic parameters on conditioning efficiency such as the maximum shear rate  $G_{\max}$ .

## DISCUSSION AND CONCLUSIONS

This paper forms part of an ongoing research program on quarry slimes management. The work focuses on slurry conditioning systems used in European quarries. It has shown that industrial conditioning systems that use weir-based configurations can be characterized to a large extent with a small set of well-known hydrodynamic parameters. From this basic analysis, the authors have highlighted some basic notions about conditioning tank design, including the significance of the connecting pipe section on conditioning efficiency.

From a direct comparison between controlled laboratory conditioning tests and full-scale measurements, it was shown that average shear rate and conditioning time govern slimes conditioning performance to a large degree. However, the work has also shown that these basic hydrodynamic parameters are not sufficient for designing efficient conditioning systems.

Indeed, with the relatively short conditioning times and high dilution used in quarries, fine measurements obtained with a dedicated laser sizer have highlighted the fact that the industrial conditioning process is utterly dynamic, with evidence of rapid competing mechanisms of floc formation, breakage and erosion. The complexity of slimes conditioning was clearly shown through examination of the interactions between small and large floc populations detected by the laser sizer. This fine analysis has revealed that slimes conditioning, which uses short conditioning times, does not operate near equilibrium conditions. As a result, it is extremely sensitive to changes in hydrodynamic conditions. In order to derive robust schemes for designing and operating quarry slimes conditioning systems, more in-depth characterization of the hydrodynamic parameters that affect this dynamic process is necessary.

## NOMENCLATURE

$V$	conditioning volume, $\text{m}^3$
$Q_f$	volumetric flow rate, $\text{m}^3 \text{s}^{-1}$
$N$	impeller rotational speed, rpm
$\bar{G}$ (or $G$ )	mean shear rate, $\text{s}^{-1}$
$G_{\max}$	maximum shear rate, $\text{s}^{-1}$
$h$	head loss, m
$g$	gravitational acceleration, $\text{m s}^{-2}$
$d_{80}$	80% passing size, m
$d_{99}$	99% passing size or maximum size, m

### Greek symbols

$\Lambda$	macro-turbulence length, m
$\tau$	residence (or conditioning) time, s
$\rho_p$	slurry density, $\text{kg m}^{-3}$
$\mu_p$	slurry viscosity, Pa s
$\lambda$	micro-turbulence length, m

## REFERENCES

- Akers, R., 1975, *Flocculation* (IChemE, Rugby, UK).
- Argaman, Y. and Kaufman, W.J., 1970, Turbulence and flocculation, *J Sanitary Eng Div*, 26: 223–241.
- Biggs, C.A. and Lant, P.A., 2000, Activated sludge flocculation: on-line determination of floc size and the effect of shear, *Water Res*, 34(9): 2542–2550.
- Biggs, C.A. and Lant, P.A., 2002, Modelling activated sludge flocculation using population balances, *Powder Technol*, 124: 201–211.
- Connelly, L.J. and Richardson, P.F., 1984, Coagulation and flocculation in the mining industry, in *Solid/Liquid Separation and Mixing in Industrial Practice, One-day Symposium*, Pittsburgh, PA (AIChE).
- Farrow, J. and Warren, L., 1993, Measurement of the size of aggregates in suspension, in *Coagulation and Flocculation: Theory and Applications*, Dobiás, B. (ed.) (Marcel Dekker, New York, USA), pp 391–426.
- Farrow, J.B., Fawell, P.D., Johnston, R.R.M., Nguyen, T.B., Ruddman, M., Simic, K. and Swift, J.D., 2000, Recent developments in techniques and methodologies for improving thickener performance, *Chem Eng J*, 80: 149–155.
- Flesch, J.C., Spicer, P.T. and Pratsinis, S.E., 1999, Laminar and turbulent shear-induced flocculation of fractal aggregates, *AIChE J*, 45(5): 1114–1124.
- Gregory J., and Kayode T.O., 1989, On-line monitoring of polymer conditioning, in *Flocculation and Dewatering*, Moudgil, B.M. and Scheiner, B.J. (eds) (Engineering Foundation, New York, USA), pp 645–655.
- Heiskanen, K. and Laapas, H., 1979, in *Proceedings of the XIII IMPC*, Vol 1, pp 183–204.
- Hogg, R., 1980, Flocculation problems in the coal industry, in *Fine Particles Processing*, Somasundaran, P. (ed.) (AIME), pp 990–999.
- Hogg, R., 1992, Agglomeration models for process design and control, *Powder Technol*, 69: 69–76.
- Hogg, R., Bunnau, P. and Suharyono, H., 1993, Chemical and physical variables in polymer-induced flocculation, *Miner Metall Proc*, May: 81–85.
- Keys, R.O. and Hogg, R., 1979, Mixing problems in polymer flocculation, *Water 1978*, AIChE Symposium Series, Vol 75 (AIChE), pp 63–72.
- Klimpel R.C. and Hogg, R., J., 1986, Effects of flocculation conditions on agglomerate structure, *J Colloid Interface Sci*, 113: 121–131.
- Parker, D.S., Kaufman W.J. and Jenkins, D., 1972, Floc breakup in turbulent flocculation processes, *J Sanitary Eng Div*, 98: 79–99.
- Pendse, H.P., 1989, Development of an on-line flocculation analyzer for the process industries, in *Flocculation and Dewatering*, Moudgil, B.M. and Scheiner, B.J. (eds) (Engineering Foundation, New York, USA), pp 657–662.
- Penney, W.R., 1985, Solid-liquid systems, in *SME Mineral Processing Handbook*, Weiss, N.L. (ed.) (Engineering Foundation, New York, USA), Vol 1, pp 8-3–8-7.
- Rey, P.A., 1989, The effect of water chemistry on the performance of anionic polyacrylamide-based flocculants, in *Flocculation and Dewatering*, Moudgil, B.M. and Scheiner, B.J. (eds.) (Engineering Foundation, New York, USA), pp 195–214.
- Spicer, P.T., Pratsinis, S.E., Raper, J., Amal, R., Bushell, G. and Meesters, G., 1998, Effect of shear schedule on particle size, density, and structure during flocculation in stirred tanks, *Powder Technol*, 97: 26–34.
- Spielman, L.A., 1977, Hydrodynamic aspects of flocculation, in *The Scientific Basis of Flocculation*, Ives, K.J. and Freshwater, D.C. (eds) (NATO Advanced Study Institute, Christ's College, Cambridge, UK).
- Tomi, T. and Bagster, D.F., 1978, The behaviour of aggregates in stirred vessels, part I—theoretical considerations on the effects of agitation, part II—an experimental study of the flocculation of galena in a stirred tank, *Trans IChemE*, 56: 1–18.
- Waters, A.G., 1992, Clarification and thickening, in *Advanced Coal Preparation Monograph Series*, Swanson, A.R. and Partridge, A.C. (eds.) (Australian Coal Preparation Society), Vol V, Part 12.

## ACKNOWLEDGEMENTS

The authors wish to express their gratitude to SNF FLOERGER and SOTRES Lamex for their continuing technical support.

## ADDRESS

Correspondence concerning this paper should be addressed to Dr F. Bourgeois, BRGM, Environment and Process Division, 3, Av. Claude Guillemin, 45060 Orleans, France.  
E-mail: f.bourgeois@brgm.fr

The paper was presented at the 9th Congress of the French Society of Chemical Engineering held in Saint-Nazaire, France, 9–11 September 2003. The manuscript was received 7 February 2003 and accepted for publication after revision 8 September 2003.